CHEMICAL ENGINEERING TRANSACTIONS, Volume 11, 2007
Edited by Sauro Pierucci
 ISBN 978-88-95608-00-6

Particle Migration in a Stirred Vessel at Low Reynolds Numbers

N. Nishioka[1], Y. Tago[2], T. Takigawa[3], M. N. Noui-Mehidi[4], J. Wu[4], N. Ohmura[2]
1 Graduate School of Science and Technology, Kobe University,
1-1 Rokkodai, Nada, Kobe 657-8501, Japan
2 Department of Chemical Science and Engineering, Kobe University,
1-1 Rokkodai, Nada, Kobe 657-8501, Japan
3 Process Research Laboratories, Kashima Plant, Eisai Co. Ltd.,
22-Sunayama, Hasaki-machi, Kashima, Ibaraki 314-0255, Japan
4 Energy and Thermofluids Engineering, CSIRO,
P.O. Box 56 Highett, Victoria 3190 Australia

Flow patterns and particle migration in a stirred vessel with no baffle plates were investigated experimentally and numerically at low Reynolds Numbers. The trajectories of resin particles having the density of 1377 – 1663 kg/m^3 and the diameter of 5 mm were analyzed using image processing. Numerical simulation using a commercial CFD code (R-FLOW) was also performed to elucidate the mechanism of particle migration in a laminar flow in the stirred vessel. The secondary circulation flow depending on the impeller off-bottom clearance affects the mixing and particle migration. At even the lowest Reynolds number (Re=10), almost all particles whose density was larger than the fluid were drawn into isolated mixing regions (IMRs) for the lowest off-bottom clearance. A nonlinear dynamic analysis revealed that those particles were finally captured in a phase-locked orbit within IMR.

1. Introduction

Mixing is one of the most important unit operations in chemical and biochemical industries. There are two flow states in a vessel, i.e. laminar flow and turbulent flow. Although turbulent flow condition is efficient for mixing, some situations require laminar mixing condition, e.g. polymerization reactions using high viscosity materials and biotechnological applications using shear-sensitive materials such as mammalian cells and proteins. Laminar flow has, however, some problems for global mixing. In laminar flow, there are segregated mixing regions in the form of troidal vortices above and below an impeller. These regions, called isolated mixing regions (IMR), do not exchange materials with outside active mixing regions (AMR). Much attention has been paid to how to efficiently eliminate IMRs at low Reynolds numbers. Yao *et al.* (1998) suggested an unsteady impeller operation that quickly achieves uniform mixing. The impeller off-bottom clearance affects the circulation inside stirred tanks for both single- and multi-phase flows, with consequent effects on mixing characteristics. Galletti *et al.* (2003) observed the flow pattern transition with impeller clearance variations in a stirred vessel with spectral and wavelet analysis. The authors recently observed that

these particles were captured within IMRs at low Reynolds numbers. This phenomenon of particle migration may conceivably affect laminar mixing characteristics in a stirred vessel also. In this study, therefore, the particle migration was investigated experimentally and numerically in laminar flow.

2. Experimental

2-1 Flow visualization and trajectories of particles

Figure 1 shows schematic diagram of the experimental apparatus. The mixing system consists of a cylindrical flat-bottom vessel without baffle of acrylic resin and a 4-bladed Rushton turbine. Geometrical details of the apparatus are also shown in Figure 1. The ratio of impeller off-bottom clearance C to the tank diameter C/T was changed from 0.143 to 0.5. The work fluid was glycerine (ρ = 1260kg/m^3, μ = 1.4Pa・s). To investigate the flow state in the vessel, decolorization reaction by acid-basic neutralization was used. Mixing process was induced to fluoresce using a plane sheet of laser light.

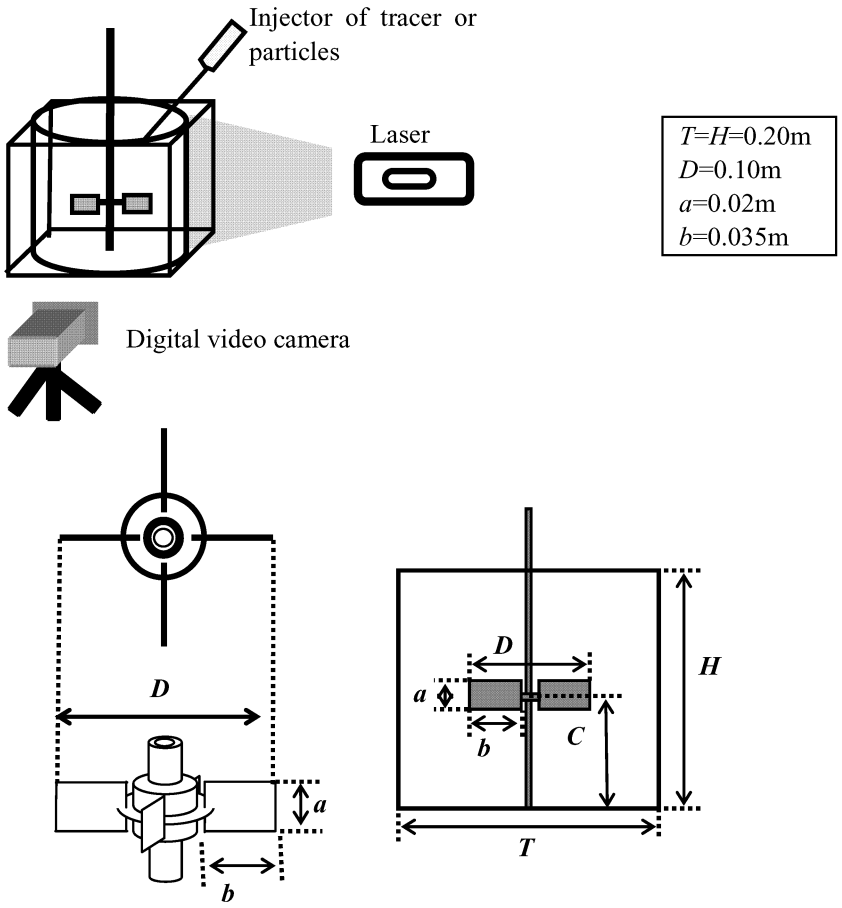

Fig.1 Scheme of experimental apparatus and impeller

The segregated regions were taken by digital video camera. The trajectories of resin particles were analyzed using image processing. Particles have density from 1377 to 1663 kg/m^3 and diameter of 5 mm. After steady state, 10 particles were placed on the upper surface located at 5 cm away from the impeller axis.

2-2 Numerical simulation

Numerical simulation is performed to obtain the velocity vector in a vessel and the trajectory of particles. The commercial CFD code R-FLOW (R-FLOW Co., LTD.) was used. The number of computational mesh is 60 x 60 x 60 in r, θ, z components, respectively. The geometry and boundary conditions for the simulation were the same as those for the experiment. The flow field was obtained by solving the three-dimensional Navier-Stokes equations and the mass conservation for incompressible fluid based on the finite volume method.

3. Results and Discussion

3-1 Flow patterns

Figure 2 shows typical examples of flow patterns. When C/T >0.2, the discharged stream from the impeller horizontally moves toward the wall and splits into two streams. Finally, there are two stable streams and IMRs above and below the impeller in the vessel, as shown in Fig.2 a). In the present work, this flow pattern is named “double-loop flow pattern (DLFP)”. On the other hand, when C/T = 0.143, the discharged stream from the edge of impeller moves toward the bottom owing to the Coanda effect and continues upwards to form a large single circulation loop named “single-loop flow pattern (SLFP)”, as shown in Figure 2 b). Although one large vortex was generated above the impeller, there was a small vortex below the impeller. These flow features are in quantitative agreement with Nienow’s observation (1968). When 0.143 < C/T < 0.2, although the discharged stream was inclined downwards somewhat, it reached the sidewall and split into two streams. Consequently, the flow pattern is similar to DLFP. In order to distinguish this flow pattern from DLFP, this flow pattern is referred to as “transitional double-loop flow pattern (TDLFP)”. Figure 3 shows the cross-sectional area of IMR measured in right half plane using Gray-val (Library Co.,LTD.) plotted against C/T. The area was measured at 120 min after injecting the acidic solution at Re=10 and 15 min at Re=30, respectively. When 0.2 < C/T < 0.5, the total area of IMR decreases but the upper area of IMR is almost constant. This means only the lower area of IMR becomes small owing to the decrease of the circulation area. On the other hand, when 0.143 < C/T <0.2, the upper area of IMR also decreases. Finally, the total area of IMR is the smallest in the case of C/T=0.143 by the disappearance of the lower IMR.

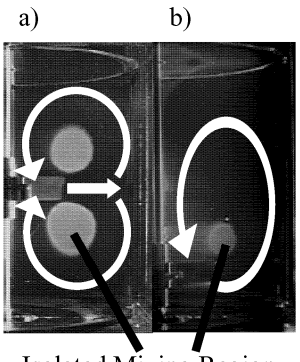

Fig.2 Flow patterns at Re=10; a) double-loop pattern (C/T = 0.5) and b) single-loop pattern (C/T = 0.143)

In order to investigate the difference between DLFP, TDLFP and SLFP, numerical simulations were conducted. Figure 4 shows velocity vector field for DLFP and SLFP.

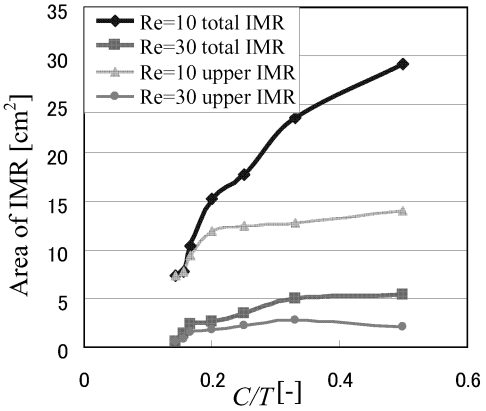

Fig.3 Area of IMR against *C/T*

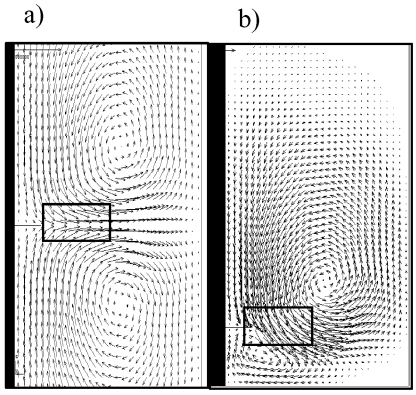

Fig.4 Velocity vector fields in a vertical right half plane at *Re*=30, a) *C/T*=0.500 and b) *C/T*=0.143

The vector field shows good agreement with the results of flow visualization experiments. When *C/T* = 0.5, the vectors discharged from the edge of impeller horizontally moved towards the bottom and generated two vortices in the vessel. In the case of *C/T* = 0.143, the discharged stream moved towards the bottom owing to the Coanda effect and one large vortex was generated. Compared with DLFP, strong vorticity can be found in SLFP. The result of this strong vorticity is a decrease in the upper area of IMR. Although SLFP drastically decreases the area of IMR, the velocity at the corner of the vessel is fairly weak.

3-2 Particle migration

The observation of particle motions was conducted by placing 10 resin particles on the upper surface located at 5 cm away from the impeller axis. In the present work, particle migration was mainly observed at *Re* = 10. When *C/T* = 0.500 (DLFP), about half the particles were captured on a torus orbit within IMRs and kept traveling around the impeller axis. On the other hand, the rest of the particles sunk to the bottom of vessel. They remained on the bottom and kept travelling around the impeller axis. When *C/T* = 0.143, a few particles were directly captured just after injection. The rest of the particles sunk to the bottom first. Then owing to the strong vortex motion of the secondary circulation formed below the impeller, those particles were whirled up again and captured in a torus orbit within the lower IMR. In order to clarify particle orbit within IMR, the present work constructed Poincaré sections corresponding to an arbitrary plane cutting a torus orbit transversally in the manner of the nonlinear dynamic theory. As illustrated in Figure 5, the primary and secondary circulation flow directions are defined as ϕ-direction and θ-direction, respectively. As shown in Figure 5, the return angle θ_n can be associated with the particle motion on the torus orbit. By selecting some arbitrary zero angle on the Poincare section, the angle θ_n made by successive returns can be specified. A θ-map (circle map) can be obtained by plotting the (n+1)th angle against nth. Figures 6 and 7 show a Poincaré section and θ-map obtained at *C/T*=0.5 and 30 minutes after injection, respectively. These figures clearly show that the particle motion covers the full surface of the torus orbit. This result indicates that the ratio of the time of

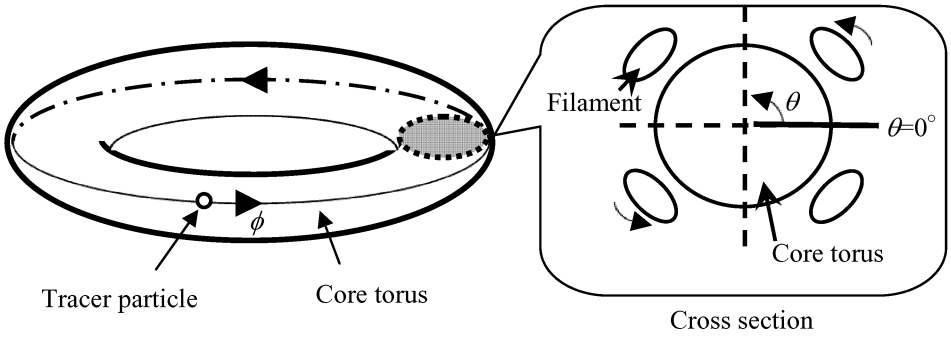

Fig.5 Definition of θ-and ϕ-directions

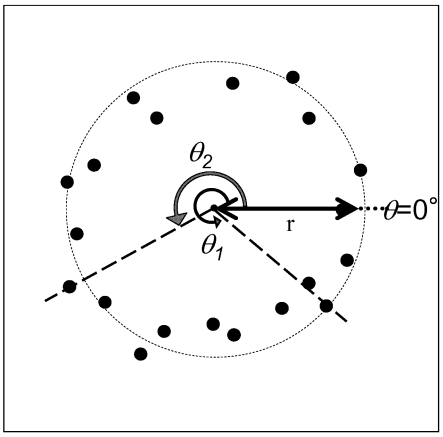

Fig.6 Poincaré section of particle orbit (after 30 minutes)

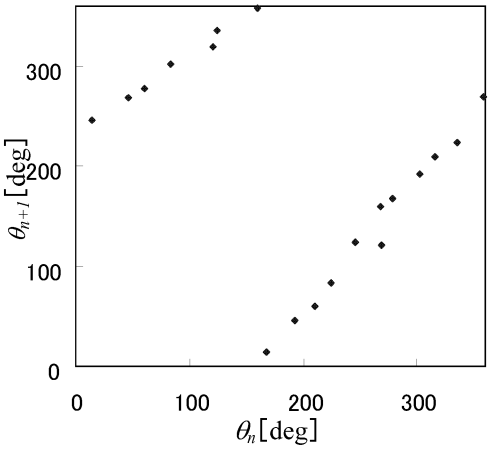

Fig.7 θ-map (after 30 minutes)

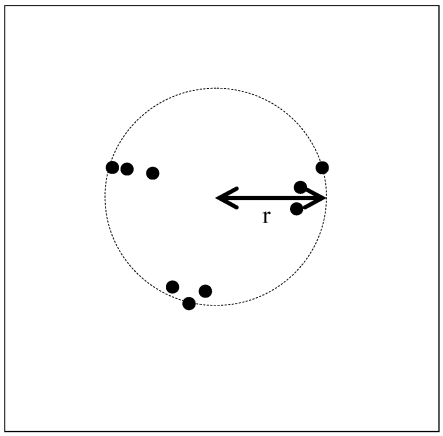

Fig.8 Poincaré section of particle orbit (after 120 minutes)

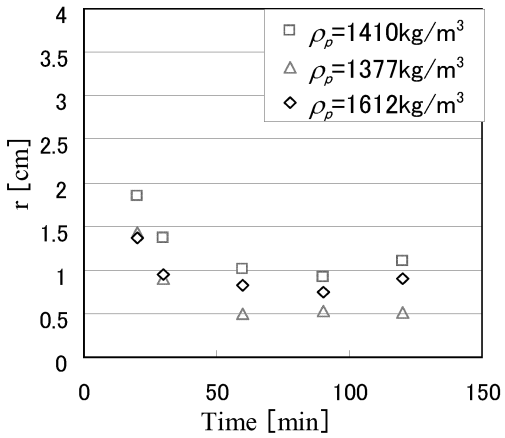

Fig.9 Radius vs. time

period for one round of a tracer particle in θ-direction, P_θ, to the time for one round in ϕ-direction, P_ϕ, is irrational. Figure 8 shows Poincaré section obtained at C/T=0.5, 120 minutes after injection. As can be seen from Figure 8, the cirular orbit on the Poincaré section converges on three discrete regions. This indicates that P_θ / P_ϕ is rational and that the particle motion becomes phase locked on the torus. Ohmura *et al.* (2003) revealed that the ratio of the time period for one round of a filament around the core IMR in θ-direction to the time for one round of a tracer particle in the filament in ϕ-direction is rational. It can be, therefore, considered that particles initially move on the surface of the core torus and finally move in a filament within IMR.

As also shown in Figures 6 and 8, by determining the origin of the circular orbit on the Poincaré section, the radius of particle rotation can be measured. Figure 9 shows the radius of particle rotation plotted against time, with particle density. Each particle has settled on a certain torus orbit about 50 minutes after particle injection. As shown in Figures 6 and 8, when particles move on the surface of the core torus, the radius decreases. After being captured within a filament existing around the core torus, the radius is almost constant. Figure 9 also shows that the final limit torus orbit is not unique. No relation between the final orbit and particle density, however, can be found so far.

4. Conclusion

Particle migration in a stirred vessel with no baffle plates was investigated experimentally and numerically at low Reynolds numbers. When $C/T > 0.2$, the discharged stream from the edge of impeller was directed horizontally towards the wall where it splits into two streams that generate two stable vortices to form IMRs. On the other hand, when $C/T < 0.2$, the discharged stream from the edge inclined downwards owing to Coanda effect. Although the stream reached the side wall and split into two streams, the secondary circulation above the impeller was so strong that the area of IMR drastically decreased. When 10 particles were placed on the upper surface located at 5 mm away from the impeller axis, about half of the particles were captured within IMRs at $C/T = 0.5$. At even the lowest Reynolds number (Re=10), almost all particles whose density was larger than the fluid were drawn into the lower IMR owing to the strong vorticity of the second circulation in the case of $C/T = 0.143$. A nonlinear dynamic analysis revealed that the particles were finally captured in a phase-locked orbit within the IMR. It can be considered that this phase-locked orbit exists in a filament around the core torus of the IMR.

5. Reference

Galletti, C., Brunazzi, E.,Yianneskis, M. and Paglianti,A., 2003, Chem. Eng. Sci., 58, 3859 – 3875

Nienow, A. W., 1968, Chem. Eng. Sci., 23, 14553-1459

Yao, W. G., Sato H., Takahashi, K. and Koyama, K., 1998, Chem. Eng. Sci., 53, 3031-3040

Ohmura, N., Makino T., Kaise, T. and Kataoka, K., 2003, J. Chem. Eng., 36, 1458-1463